Molecular functional analyses of larval adhesion in a highly fouling invasive model ascidian

Jiawei Cheng
Chinese Academy of Sciences
Shiguo Li
Chinese Academy of Sciences
Xi Li
Chinese Academy of Sciences
Ruiying Fu
Chinese Academy of Sciences
Xuena Huang
Chinese Academy of Sciences
Aibin Zhan (zhanaibin@hotmail.com)
Chinese Academy of Sciences

Research Article

Keywords: ascidians, papillae, biofouling, adhesion, micro-transcriptome, adhesive protein

Posted Date: April 11th, 2022

DOI: https://doi.org/10.21203/rs.3.rs-1524932/v1

Abstract

Successful papillary adhesion is the first essential step for serious ascidian biofouling in marine ecosystems; however, the mechanisms of papillary adhesion have not been fully elucidated. Here, we employed micro-transcriptome sequencing to assess the differentially expressed genes (DEGs) between papillae and remaining body in the larvae of the highly fouling invasive model ascidian *Ciona robusta*. Enrichment results for DEGs showed that papillae were adhesive structures with the combined functions of substrate recognition, environmental perception, and adhesive protein synthesis and secretion. Two candidate ascidian papilla adhesive proteins (APAPs), APAP-1 and APAP-2, were identified, expressed, and purified *in vitro*. Surface coating tests showed that APAP-1 was a cohesive protein while APAP-2 was an interfacial protein involved in the adhesion between papillae and material surface. Collectively, the obtained DEGs and adhesive proteins provide candidates to deeply understand molecular mechanisms of underwater adhesion and further develop anti-fouling strategies in marine ecosystems.

Introduction

Biofouling, the intensive colonization and adhesion of organisms on submerged substrates, has caused a series of economic and environmental issues in marine ecosystems (Salta et al. 2010; Madin and Ching 2015; Bannister et al. 2019). So far, the number of marine fouling species has reached > 4,000, among which ascidians are one of the dominant taxa due to their enormous adhesion biomass on the surfaces of underwater facilities, causing significantly negative effects on both industries and local environments (Aldred and Clare 2014). For instance, fouling ascidians were the main contributor to the production loss of cultured sea cucumbers and shellfish such as oysters, clams, and scallops in the Pacific, Atlantic, and Indian Oceans, and the economic loss for the control of fouling species such as ascidians in aquaculture alone was approximately US $1.5–3 billion per year (Lambert 2007; Davis and Davis 2010; Adams 2011; Fitridge et al. 2012). In addition, ascidian biofouling was also one of the additional costs for hull maintenance and fuel consumption in the shipping industry (Aldred and Clare 2014). Ecologically, fouling ascidians can reduce species richness and change biodiversity patterns of benthic communities in local marine ecosystems (Castilla et al. 2004; Zhan et al. 2015). For example, biofouling by the ascidian *Ciona intestinalis* in San Francisco Bay resulted in sharp decreases in biomass of other sessile species such as Bryozoa and Porifera (Blum et al. 2007). Although a series of encouraging progress have been made in anti-fouling in the past decades (Salta et al. 2010; de With 2018), unfortunately ascidian fouling has not been effectively controlled, which can be seen from an indisputable fact that the negative influence has been increasing in frequency and area affected (Aldred and Clare 2014; Zhan et al. 2015). Therefore, there is an urgent need to develop effective anti-fouling strategies to maintain the health and integrity of global marine ecosystems and sustainable development of marine industries.

The key step in formulating anti-fouling strategies is to successfully reveal the detailed mechanisms underlying rapid and strong adhesion to underwater surfaces (Prendergast 2009). Ascidian adhesion begins with swimming larvae and becomes stronger in adults. Solitary adult ascidians with high fouling abilities rely mainly on their special adhesive organ termed stolon to adhere firmly to various underwater surfaces (Hirose and Akahori 2004; Ueki et al. 2018). Studies have showed that ascidian stolon was insensitive to the changes of marine environments, even some chemicals for anti-fouling (Hirose and Akahori 2004; Li et al. 2021a), thus increasing great uncertainty and difficulty to eradication. The adhesion of swimming larvae is a signal to initiate subsequent metamorphic development of ascidians (Matsunobu and Sasakura 2015). As a result, if larval adhesion fails, ascidians are not able to start metamorphosis to complete their life history, and finally die off. Therefore, when comparing with high difficulties in control and management of fouling ascidians at the adult stage, the interruption of adhesion at larval stages represents a direct, cost-effective, and efficient way to solving biofouling problems by ascidians.

The adhesion of ascidian larvae depends on their specific structures at the anterior end of the head, which are composed of three cup-shaped translucent papillae. Each papilla consists of three distinct types of cells: axial columnar cells (ACCs), lateral primary sensory neurons (PSNs), and central collocytes (CCs). ACCs and PSNs play important roles in substrate recognition, while CCs are involved in the synthesis of adhesive proteins, which are eventually transported to hyaline caps prior to the papilla (Zeng et al. 2019a). Available evidence suggests that the adhesive proteins synthesized in the CCs of the papilla can be quickly released to substrate surfaces to achieve underwater adhesion when papillae successfully contact with the surfaces of proper underwater substrates (Cloney 1977; Pennati et al. 2007; Caicci et al. 2010; Zeng et al. 2019b). However, in contrast to the detailed knowledge of structure of ascidian papillae, little is known about the protein composition of these papillary secretions and no associated adhesive protein has been successfully identified from papillae. The underlying molecular mechanisms of these protein adhesion, which are essential for formulating anti-fouling strategies against ascidian larvae, are also largely obscure.

One of the main reasons for the lack of adhesive protein information is the small size of ascidian larvae (only 20 μm in length), largely impeding the isolation and identification of adhesive proteins from its tiny sub-structures. The micro-transcriptome sequencing technique developed recently can help solve this technical problem because it allows for the use of total RNA isolated from micro-samples for library construction and sequencing (Cao et al. 2019). Using this technique, the cDNA libraries of two micro-samples, the papillae and the remaining body of *Ciona robusta* larvae, were constructed in this study. *C. robusta* was used as the experimental model here mainly due to its strong fouling characteristics at both larvae and adult stages in marine ecosystems (Aldred and Clare 2014; Zhan et al. 2015). In particular, this species is highly invasive, and the strong fouling capacity has caused severe economic and ecological problems globally (see review by Zhan et al. 2015). In contrast to its negative effects, the well sequenced and annotated small genome (123 Mb), as well as abundant genetic resources, makes this species a good model for answering multi-disciplinary questions (Zhan et al. 2015; Satou et al. 2019), thus facilitating detailed gene expression and protein function analyses in this study. After comparative transcriptomic analyses, we characterized differentially expressed genes (DEGs) between the two micro-samples, and subsequently genes encoding for candidate papilla adhesive proteins were identified form papillae and then expressed *in vitro*. The adhesive abilities of these purified proteins were further verified by surface coating analyses. Here, we aim to understand specific genes and proteins involved in papillary adhesion, and the results obtained in this study are expected to provide a reference to fully understand the mechanisms of underwater adhesion and develop anti-fouling strategies in marine ecosystems.

Materials And Methods

Ascidian collection and artificial fertilization

C. robusta adults (6.0 cm in length) were collected from a marine shellfish farm in Dalian, Liaoning Province, China (38°49′13″ N, 121°24′20″ E) in September 2020. All collected ascidians were rapidly transported to the laboratory and temporarily acclimated in a 1000 L circulating aquarium using the same conditions (20 ± 1°C, 30 ± 1 psu, and pH 8.10 ± 0.05) as the sampling site for three days. During acclimation, each hundred ascidians were fed daily with 10g dried algae powder mixture of *Chlorella sp.* and *Spirulina sp.* until sperm duct and oviduct appeared. Six matured individuals were dissected with sterilized surgical blades to obtain sperm and eggs. The collected eggs were temporarily stored in a collection tube, while the collected sperm was added into a 1.5 mL centrifuge tube containing 1 mL pre-cooled sterilized seawater. Before fertilization, the eggs were rinsed with sterilized seawater for 1 minute to remove their chorion surfaces. A total of 0.5 mL sperm was then added into the collection tube with 1000 eggs for artificial fertilization. After fertilization for 10 minutes, the eggs were rinsed slowly with sterilized seawater to remove excess sperm and incubated in a Petri dish. The incubation condition was controlled at 18°C ± 1, 30 ± 1 psu, and pH 8.10 ± 0.05 in darkness. The fertilized eggs were incubated for 24 h to obtain swimming larvae, which were finally collected for the following RNA extraction and transcriptome sequencing. The overall scheme of our experiment is shown in Fig. 1.

Micro-dissection and RNA extraction

The swimming larvae were transferred into 100 μL sterilized seawater dropped on a glass slide. A tungsten needle with tip diameter of 1 μm (HengMi, Shanghai, China) was used to dissect the papillae and body of *C. robusta* swimming larvae under an optical stereomicroscope (Olympus SZ51, Tokyo, Japan). The detailed dissecting position on swimming larvae is shown in Fig. 1. The dissected papillae and body were distributed into two 2 mL lyophilization tubes. Three biological replicates were set up for all the papillae and body samples, respectively. All samples were snap-frozen with liquid nitrogen and then preserved at -80°C.

The collected samples were pre-fragmented using an ultrasonic cell disruptor (Scientz JY92-ⅡDN, Ningbo, China) with Φ Ⅱ horn after being mixed with 350 μL cell lysis buffer from a RNeasy Micro Kit (Qiagen, 74001, Dusseldorf, Germany). The whole ultrasound process was conducted on ice with parameters of 20 kHz, 60 W, and 2 minutes (1s ON and 3s OFF). The total RNA was extracted from the disrupted papillae and body samples using a RNeasy Micro Kit following the manufacturer's instructions. The possible DNA contamination was removed by DNase I provided by the kit.

Transcriptome sequencing

A total of six cDNA libraries were constructed based on the extracted RNA samples using the Smart-seq2 method (Picelli et al. 2014). These libraries were subsequently sequenced using the illunima MiSeq platform in CapitalBio Technology Company in Beijing, China. All the raw sequencing data were deposited in the National Centre for Biotechnology Information (NCBI) under the accession number (SUB10810372). The quality of reads in raw data was evaluated by FastQC (http://www.bioinformatics.babraham.ac.uk/projects/fastqc/). TRIMMOMATIC (Bolger et al. 2014) was used to filter low-quality reads and trim adapters. After filtration, HiSAT2 (Kim et al. 2015), FeatureCounts (Liao et al. 2014), and DEseq2 (Love et al. 2014) were employed for mapping the *C. robusta* genome and identifying differentially expressed genes (DEGs). All the above analyses were carried out according to the default parameters in corresponding programs and software. The DEGs were screened by comparing the changes in gene expression levels between the papillae and body samples. Briefly, the genes with reads less than 10 in more than half of the samples in the raw data were firstly excluded. The DEGs were identified from the remaining genes using the cut-off criteria of p-value < 0.05 and fold change > 2. The obtained DEGs were further employed to perform Gene Ontology (GO) and Kyoto Encyclopedia of Genes and Genomes (KEGG) enrichments using TBtools software (Chen et al. 2020) with default parameters.

Real-time quantitative PCR verification

To verify the gene expression results obtained from transcriptome analysis, the same RNA samples used for transcriptome sequencing were also used to synthesize the first-strand cDNA using a reverse transcription kit (Takara, Tokyo, Japan) following the manufacturer's instructions. A total of 5 up-regulated and 3 down-regulated DEGs were randomly selected from the transcriptome sequencing results to verify their expression changes by real-time quantitative PCR (RT-qPCR). The RT-qPCR was conducted using the LightCycler® 96 instrument (Roche, Basel, Switzerland) and a FastStart Essential DNA Green Master Kit (Roche) following the manufacturer's instructions and the obtained first-strand cDNA was used as the PCR template. The detailed sequence and primer information for these selected DEGs were listed in the Table S1. The *β-actin* of *C. robusta* was used as the reference gene (Fujikawa et al. 2010), and the relative fold changes in eight DEGs were calculated following the $2^{-\Delta\Delta CT}$ method (Livak and Schmittgen 2001).

Adhesion-related gene screening

The genes encoding papilla adhesion-related proteins were screened from the DEGs with the fold changes of genes expression > 4 between papillae and body. The remaining genes were further screened according to the common characteristics of adhesive proteins in marine organisms summarized by previous literature (Silverman and Roberto, 2007; Li et al. 2021b). Briefly, the most abundant amino acids were glycine, leucine, tyrosine, serine, threonine, cystine, or arginine and the percentages were greater than 10%. Meanwhile, the conserved domains such as thrombospondin-1 (TSP-1), von willebrand type C (vWC), or epidermal growth factor (EGF) must be included. Additionally, repetitive sequence and posttranslational modification (phosphorylation, glycosylation, hydroxylation) were considered as optional screening criteria. The ProtParam and ProtScale online programs in Expasy platform (https://www.expasy.org/) were used to predict the molecular size, charge, and hydrophobicity of candidate adhesive proteins deduced from the screened genes. SMART (http://smart.embl-heidelberg.de/), SignalP (http://www.cbs.dtu.dk/services/SignalP/), NetPhos-3.1 (https://services.healthtech.dtu.dk/service.php?NetPhos-3.1), SOPMA (https://npsa-prabi.ibcp.fr/cgi-bin/npsa_automat.pl?page=npsa_sopma.html), and PHYRE2 (http://www.sbg.bio.ic.ac.uk/phyre2/html/page.cgi?id=index) were employed to predict the conserved domains, signal peptides, phosphorylation sites, and spatial structure of candidate adhesive proteins, respectively.

Protein recombination and purification

The full-length open reading frames (ORFs) of the genes encoding for candidate papilla adhesive proteins were synthesized *in vitro*. The synthesized sequences were inserted into the cleavage site of an expression plasmid pCMV3-C-His Negative Control Vector with a C-terminal decahistidine (10 × His) tag. The recombinant vectors were then transformed into the mammalian cell HEK293 expression system to produce recombinant proteins. After seven days, the cells were lysed using ice-cold modified RIPA lysis buffer with cocktail of protease inhibitors (Sigma, Burlington, USA). The Ni affinity chromatography columns (GE 17-0409-01, Uppsala, Sweden) were used for adsorbing proteins, after which the target proteins were gathered by gradient elution with imidazole. The concentration and purity of adhesive proteins were determined by UV spectroscopy with optical density value at 280 nm and sodium dodecyl sulfate polyacrylamide gel electrophoresis (SDS-PAGE), respectively.

Adhesive ability test

Surface coating experiment was carried out on different materials to test the adhesive abilities of recombinant proteins according to a previous method with minor modifications (Li et al. 2019). Polyvinyl chloride (PVC), acrylonitrile-butadiene-styrene plastic (ABS), mica, stainless steel, aluminum, hydrophilic glass, and hydrophobic glass were selected as the substrate materials. The concentration of all recombinant proteins was adjusted to 0.22 mg/mL before tests and the test volume was 10 μL. The Cell-Tak (Corning Life Sciences, New York, MA, USA), a commercial adhesive mixture of mussel foot proteins, was used as the positive control, while the bovine serum albumin (BSA, Yuanye, Shanghai, China) was used as the negative control. The PVC material was further used to estimate the effects of metal ions (calcium, magnesium, sodium, and potassium ions) and charged amino acid (glutamate and arginine) on the adhesive abilities of recombinant proteins. For all tests, the spots of proteins were stained using Bradford assay (Solarbio, Beijing, China) after dropping on the material surfaces for 12 h. The stained spots were photographed with a digital camera (E-P7, Olympus, Tokyo, Japan) and obtained images were submitted to the ImageJ software (Hartig 2013) for gray analysis. The peak plot and relative gray value were used to represent the adhesive abilities of recombinant proteins.

Statistical analysis

The difference between the relative gray values of spots in adhesive ability analysis was evaluated using one-way analysis of variance (ANOVA) with the significance levels at $*p < 0.05$ and $**p < 0.01$. The gene expression changes from DEGs analysis were represented by volcano plot. The significantly enriched functional clusters in GO and KEGG analyses were selected for plotting using ggplot2 in the R package (Wickham et al. 2016). The rest of the plots were drawn using Adobe Illustrator CS5.

Results

Transcriptome sequencing

On average, 28.38 million paired-end reads were produced by sequencing the cDNA libraries constructed from the papillae and body samples. After adapter cleaning, quality trimming, and length filtering, a total of 28.00 million clean reads (98.67% of the total reads) were obtained. For the papillae cDNA library, an average of 62.75% of the quality-filtered reads were mapped to the reference genome of *C. robusta* and 2.85% of the reads were mapped to multiple regions of this genome. For the body cDNA library, the correspondence mapping ratios were 75.47% and 3.61%, respectively (Table S2). These multiple mapping reads were excluded in the subsequent analysis by HiSAT2. A total of 18,191 genes were annotated into the genome of the ascidian *C. robusta* (Satou et al. 2019), and an average of 17,633 (±173) genes were found to be expressed in six samples.

Identification of DEGs

After filtering the low-expressed genes, a total of 16,001 genes were obtained for subsequent DEGs analysis. A total of 5,051 genes were found to be differentially expressed in both papillae and body samples, with 1,875 genes were highly expressed in papillae and 3,176 genes were highly expressed in body (Fig. S1; Table S3). Analysis showed that the fold changes for the DEGs in RT-qPCR and transcriptome sequencing had good correlations, confirming the accuracy and validity of our transcriptome sequencing results (Fig. S2).

Functional enrichment of DEGs

A total of 1,875 genes highly expressed in papillae compared with body were arranged for GO and KEGG enrichments. A total of 174 terms were obtained from GO enrichment and 20 terms were significantly enriched (Fig. 2a; Table S4). In the biological process classification, the DEGs were annotated to the terms ‘excretion’, ‘calcium ion transport’, ‘detection of external stimulus’, ‘face morphogenesis’, ‘protein dephosphorylation’, ‘aminoglycan catabolic process’, and ‘multivesicular body organization’. In the cellular component classification, the DEGs were enriched into the terms ‘basement membrane’, ‘photoreceptor outer segment’, ‘external encapsulating structure’, ‘pseudopodium’, ‘non-motile cilium’, and ‘neuron projection membrane’. In addition, the terms ‘serine hydrolase activity’, ‘transmission system’, ‘iron ion’, and ‘proteoglycan and glycosaminoglycan binding’ were enriched into the classification of molecular function. Taken together, the enriched GO terms could be divided into four categories including neural recognition, environmental perception, metabolism, and ion transport.

The KEGG enrichment results could also be divided into four categories: neural recognition, environmental perception, metabolism, and ion transport (Fig. 2b, Table S5). The pathways ‘serotonergic synapse’ and ‘neuroactive ligand-receptor interaction’ were enriched in neural recognition category. The pathways ‘sensory system’ and ‘interaction of environmental information processing’ were associated with environmental perception. The metabolism category included ‘xenobiotics biodegradation’, ‘linoleic acid’, ‘purine’, and ‘nucleotide and arachidonic acid’ pathways. The ‘calcium signaling pathway’ was classified into the ion transport category. The KEGG pathways with higher values of rich factor were ‘non-homologous end-joining’, ‘linoleic acid metabolism’, and ‘ovarian steroidogenesis’ (Table S5).

Genes involved in papillary adhesion

A total of six genes, encoding candidate papilla adhesive proteins with molecular size ranging from 18.54 kDa to 116.29 kDa were identified (Table 1). The proteins encoded by these genes were typically characterized by a high proportion of serine, cysteine, glycine, and threonine, while most of these proteins had a proportion of hydrophobic amino acids such as leucine. Functionally conserved domains such as TSP-1, vWC, and EGF associated with the underwater adhesion of marine fouling organisms were distributed in the sequences of candidate papilla adhesive proteins. Some proteins were predicted to be of repetitive sequences, including TSP-1 and LDLa (cysteine-rich) repetitive sequences in 'SCO-spondin' (Gene id: KY.Chr1.200.v3.ND3-3), Fibronectin type 1 (FN1) repeat sequence in 'Chordin-like protein 1' (Gene id: KY.Chr10.1268.v1.ND1-1), and several internal repeats in 'Protein delta homolog 2' (Gene id: KY.Chr11.146.v1.SL1-1). In addition, some specific domains were also found in these candidate papilla adhesive proteins. The 'Sushi, von Willebrand factor type A, EGF and pentraxin domain-containing protein 1' (Gene id: KY.Chr10.1028.v1.nonSL5-1) possessed an antimicrobial peptide-like domain, a protease activity inhibitory structural domain Somatomedin-B (SO) and a Bowman-Birk domain (BowB). Similarly, there was a leucine-rich SCAN domain in 'Fibronectin' (Gene id: KY.Chr2.475.v2.SL2-1), a cysteine-rich domain Defensin (DEFSN) and an ADAM Cysteine-Rich domain (ACR) in 'Chordin-like protein 1'.

In addition to the genes directly associated with underwater adhesion, two genes, 'opsin 1, long wave sensitive' (*OPN1LW*, KY.Chr1.1186.v2.ND1-2) and 'G protein-coupled receptor 84' (*GPR84*, KY.Chr7.1150.v1.ND1-1), we screened on those that might be involved in neural perception in papillae (Table 1). Both proteins encoded by these genes had high percentage of leucine and carried 7 transmembrane receptor (rhodopsin family, 7tm_1) domains.

Adhesive protein expression and purification

A total of two proteins (Gene ID: KY.Chr10.1028.v1.nonSL5-1 and KY.Chr10.1268.v1.ND1-1) were successfully expressed and purified *in vitro*. We named ascidian papilla adhesive protein 1 (APAP-1) and ascidian papilla adhesive protein 2 (APAP-2). After removing signal peptides and decahistidine tag labels, the purified product of recombinant APAP-1 had an SDS-PAGE band size of 46.47 kDa (Fig. 3a). The most abundant amino acid of this protein was Cystine, followed by Asparticacid, Glycine, and Asparagine in turn. Sequence analysis showed that APAP-1 had a large number of negatively charged amino acids (Fig. 3c). Furthermore, a total of six EGF-related domains, including one EGF, one EGF-like, and four EGF_CA domains, were found in APAP-1 (Fig. 3e). All the EGF-related domains were arranged in series with equal spacing, and there was only one amino acid spacing between two adjacent EGF-related domains. The purified product of recombinant APAP-2 had a band size of 65.01 kDa (Fig. 3b). The most abundant amino acid in this protein was Serine, followed by Cystine, Arginine, and Lysine. Many amino acids in APAP-2 are phosphorylable, especially for serine (Fig. 3d). APAP-2 contained three vWC domains in tandem (Fig. 3f), which were distributed at the positions of 13-70 aa, 123-184 aa, and 210-270 aa of this protein sequences.

Adhesive ability

Surface coating experiment showed that all the positive controls (Cell-Tak) were stained obviously and the negative controls (BSA) were not stained (Fig. 4a). The APAP-1 on all the material surfaces were not stained, while the APAP-2 on the corresponding surfaces were stained obviously. The adhesive abilities of APAP-2 on PVC, ABS, mica, stainless steel, aluminum, hydrophilic glass, and hydrophobic glass surfaces were strong, especially on aluminum surface where the color of APAP-2 spot was uniquely deeper than the corresponding positive control. There were no observed effects of metal ions on the adhesive ability of APAP-1 to PVC surface except iron. The additions of amino acids also had no interference with the adhesion of APAP-1 to PVC surface. (Fig. 4b). The iron also influenced the adhesive ability of APAP-2 on PVC surface (Fig. 4c). The changes in peak plots in all the gray analyses also showed similar trends with staining results (Fig. S3).

Discussion

In this study, we used the micro-transcriptome sequencing technique to assess the gene expression difference between the papillae and body tissues of *C. robusta* larvae. Interestingly, we obtained a large number of genes with higher expression levels in papillae when compared with body. Those identified genes were further functionally enriched into a series of terms/pathways, such as neural recognition, environmental perception, metabolism, and ion transport. Moreover, two adhesive proteins APAP-1 and APAP-2 were screened, expressed, and purified *in vitro*, and further confirmed to be associated with papillary adhesion. All these results provide essential information underlying molecular mechanisms of ascidian papillary adhesion, especially in the papillary substrate recognition, photoperception, and synthesis and secretion of adhesive proteins.

Substrate recognition

The larval adhesion of marine organisms to underwater substrates with different properties begins with their detective behaviors to substrate surfaces based on their nervous system (Prendergast 2009). In this study, functional enrichments for the up-regulated DEGs yielded many terms/pathways related to neural recognition, including 'transmitter-gated channel activity', 'excitatory extracellular ligand-gated ion channel activity', 'neurotransmitter receptor activity involved in the regulation of postsynaptic membrane potential', and 'neuron projection membrane', indicating the existing of strong neurophysiological activity in the papillae of *C. robusta*. In former studies, nervous system-like structures in papillae have been observed in the fouling ascidians including *C. intestinalis* (Imai and Meinertzhagen 2007a, b; Horie et al. 2009; Zeng et al. 2019b), *Distaplia occidentalis* (Cloney 1977), *Diplosoma macdonaldi* (Torrence and Cloney 1983), and *Botryllus schlosseri* (Caicci et al. 2010). These structures can be detected at the early tail-bud stage during embryo development by using fluorescent labelling technique, and further were thought to be involved in ascidian larval settlement and metamorphosis (Imai and Meinertzhagen 2007b; Caicci et al. 2010). In consistent with findings in those studies, our results here showed the neural recognition behaviors in papillae at the molecular level, suggesting their importance for *C. robusta* larval adhesion.

Microvilli and cilia are common structures at the protrusions of neurofunctional cells in ascidian larvae (Hotta et al. 2007). Consistently, our results at the molecular level showed that DEGs were enriched in the terms of 'non-motile cilium' and 'ciliary base' (Fig. 2a, Table S4). These structures can be found in two kinds of cells, axial columnar cells (ACCs) and rostral trunk epidermal neurons (RTENs), with different morphologies and localizations in the papilla, both of which were thought to be of neural functions (Imai and Meinertzhagen 2007b; Caicci et al. 2010; Zeng et al. 2019b). During larval adhesion, ACCs in the

papilla were functioned as mechanoreceptors contacting with substrate surfaces, while RTENs were considered as chemoreceptors that can primarily mediate metamorphic events after larval adhesion (Pennati et al. 2007). Such mechanical and chemical behaviors were observed in the larvae of ascidians *Phallusia mammillata* and *D. macdonaldi* (Torrence and Cloney 1983; Groppelli et al. 2003; Chase et al. 2016), as well as larvae of other marine adhesive organisms such as barnacles (Chaw and Birch 2009; Maruzzo et al. 2011). For example, the cyprids of barnacle had antennular setae, which were considered to be bimodal receptors with both chemo- and mechano-receptive modalities, playing important roles in sensing hydrodynamic forces and dissolving substances and substrates (Maruzzo et al. 2011). Based on our transcriptome results, the swimming larvae of *C. robusta* may also have substrate recognition ability by using these two types of cells.

Previous investigations demonstrated that light stimulus was an important environmental factor influencing the swimming behavior of larvae of marine organisms (Tsuda et al. 2003; Hirai et al. 2017). In fact, ascidian larvae had a specific pattern of swimming behaviors. In the first three hours after hatching, they swam upward, and then changed to swim or sink downwards until settlement (Svane and Young 1989). However, it is difficult to establish the relationship between light stimulation and larval adhesion of marine organisms based on such evidence. In our results, the up-regulated DEGs were enriched in the terms/pathways of 'detection of external stimulus', 'detection of light stimulus', 'photoreceptor outer segment', and 'sensory system' (Fig. 2), suggesting that the neural structures in papillae of *C. robusta* should be involved in not only substrate recognition but also environmental perception, especially for photoperception during papillary adhesion. This finding is consistent with the result of an investigation on the larvae of the ascidian *C. intestinalis*, where the genes associated with chordate eye formation were highly expressed in papillae. Meanwhile, once the expressions of these genes were inhibited, the development of papillae was disturbed and the photosensitive swimming behavior was lost, influencing papillary adhesive ability (D' Aniello et al. 2006). In addition to ascidians, photoperception behaviors during larval adhesion have also been found in other aquatic organisms such as the fouling barnacle *Balanus amphitrite* (Kon-ya and Miki 1994) and mussel *Dreissena polymorpha* (Marsden and Lansky 2011). The results obtained here, as well as supportive evidence in related species, suggest that the success and firm underwater adhesion of *C. robusta* papillae should be closely related to their recognition to substrate surfaces stimulated by light.

Adhesive protein synthesis and secretion

Once ascidian papillae successfully recognize suitable submerged substrates, they begin to secrete adhesives with proteins as the main functional components. These adhesives were synthesized by the specific cells and then transported to hyaline cap, the site at the anterior end of each papilla (Cloney 1977). Our study obtained several up-regulated GO terms related to secretion functions, including 'excretion' and 'multivesicular body organization', which were in line with the fact that the massive adhesive proteins were synthesized during papillary adhesion in other ascidians (Torrence and Cloney 1983; Caicci et al. 2010). Collectively, papillae in *C. robusta* are an important structure responsible for the synthesis, storage, and secretion of adhesive proteins.

In the fouling ascidian *C. intestinalis*, the cells with secretory functions were localized at the trailing end of the papilla with microvilli, small endocytic vesicles, and large numbers of adhesive granules (Zeng et al. 2019b). Such secretory cells were also observed in the papilla of another fouling ascidian *D. occidentalis* (Cloney 1977). Transmission electron microscope analysis illustrated the presence of two types of collocyte granules with different electron dense in papillary secretory cells. These granules were rich in adhesive proteins and wrapped in circular or oval shape by some membrane structures, playing key roles in papillary adhesion in *C. intestinalis* by granule cross-linking (Zeng et al. 2019b). Importantly, genes associated with Ca^{2+} transport were found to be expressed in collocytes, suggesting that Ca^{2+} should be involved in the functioning of granules (Pang and Südhof 2010; Zeng et al. 2019b). Similarly, the relevant terms/pathways responsible for Ca^{2+} transport were enriched in our study (Fig. 2), suggesting that Ca^{2+} may act as an essential ion to participate in the synthesis, storage, and secretion of adhesive proteins in *C. robusta* papillae.

The effective composition of adhesives in marine fouling organisms has always been the focus in the relative research fields. In our study, the up-regulated proteoglycan-related terms such as 'proteoglycan binding', 'glycosaminoglycan binding', and 'aminoglycan catabolic processes' were significantly enriched in papillae (Fig. 2a). In adhesive organisms, glycoproteins were one of the key biomacromoleculers involved in interfacial adhesion between adhesive structures/tissues/organs and substrates (Sarosiek et al. 1988; Moussa et al. 2014; Opell et al. 2019). In particular, protein glycosylation has been detected in the adhesive structures of several marine fouling organisms, such as mussel byssus (Suhre et al. 2014) and barnacle cement (Kamino et al. 2012). Element and histochemistry analyses for the papillae of *C. intestinalis* showed that the adhesive granules in collocytes contained glycoproteins (Zeng et al. 2019a). In addition, carbohydrate specific lectins could be detected in collocytes, hyaline caps, and adhesive plaques of the papillae in *C. intestinalis*, suggesting that the adhesives in larval papillae of this species contained some kinds of carbohydrate components, most likely in the forms of proteoglycans (Zeng et al. 2019b). Aminoglycans, including hyaluronic acid and heparin, are important components of proteoglycans. In the study by Zeng et al (2019a), the addition of heparin to seawater significantly reduced the adhesive rate of *C. intestinalis* larvae to the surface of plastic petri dish. The enrichments of the up-regulated GO terms 'aminoglycan', 'glycosaminoglycan', and 'heparin' in our study suggest that aminoglycans might be involved in the papillary adhesion of *C. robusta* (Table S4).

Underwater adhesion of APAPs

Two candidate proteins APAP-1 and APAP-2 involved in papillary adhesion in *C. robusta* were purified in this study. High abundance of cysteine, tandem EGF-related domain, and extremely negative electrical amino acids were the typical feature of APAP-1 sequence. The repeated cysteine residues and charged amino acids have been proved to be the important sequence structures that can regulate protein adhesion in marine fouling organisms. For example, CP-20K, an adhesive protein isolated from the barnacle cement, contained an arrangement of six repeated cysteine residues and negatively charged amino acids, which can form intramolecular disulfide bonds to act as a specific coupling agent between barnacles and calcified materials (Kamino 2001; Rocha et al. 2019). The EGF domains are also involved in mediating protein-protein and protein-metal interactions in the adhesive organs/tissues in marine fouling organisms (Li et al. 2021b). Some adhesive proteins such as mussel foot protein Mfp-2 and sea star foot protein Sfp-1 were rich in EGF domains (Hwang et al. 2010; Hennebert et al. 2014). Mfp-2 was located in the adhesive plaque rather than the cuticle of mussel byssus, providing cohesion for the plaque to stabilize byssus structure. Atomic force microscope analysis showed that although Mfp-2 cannot directly adhere to the mica surface, there were strong interactions among these protein molecules by formatting bis- or tris-DOPA-ion complexes between the EGF domains of Mfp-2 and metal ions. The additions of Ca^{2+} and

Fe^{3+} into the solution of this protein significantly enhanced these interactions, suggesting that the cohesiveness of adhesive plaque should rely on the ion complexation between EGF domains in Mfp-2 (Hwang et al. 2010). The EGF-related domains, including EGF, EGF-like, and four EGF_CA domains, account for 70% of the total protein theoretical size of APAP-1 in our study. In the surface coating experiment, the addition of Fe^{3+} could significantly increase the adhesive ability of APAP-1 to PVC surface, even to the similar adhesive strength as the positive control (Fig. 4b). In addition, the GO term 'iron ion binding' was also significantly enriched in papillae by comparing the up-regulated DEGs between different samples. These results suggest that APAP-1 may be a cohesive protein involved in papillary adhesion in *C. robusta* and it requires the participation of some specific metal ions to promote the interactions between molecules of this protein (Fig. 5).

There were three vWF-like domains in the sequence of APAP-2 in *C. robusta*. vWF domain is a conserved structure distributed in many adhesive proteins in marine fouling organisms, such as PTMP-1 in mussels, TSP-1 containing protein in oysters, and Sfp-1 in sea stars (Hennebert et al. 2014; Suhre et al. 2014; Liu et al. 2016). Another attractive feature of APAP-2 is the high serine content in its amino acid composition. Similarly to APAP-2 in *C. robusta*, the cement proteins CP-19k and CP-68k in fouling barnacles and the foot proteins Mfp-5 and Mfp-6 in fouling mussels were also rich in serine (Kamino et al. 2000; Waite 2001; Zhao and Waite 2006; Urushida et al. 2007). In addition, the phosphorylation prediction for APAP-2 showed that most serine sites in this protein could be phosphorylated. The phosphorylated serine was abundance in both mussel foot proteins Mfp-5 and Mfp-6. The phosphorylated sites in Mfp-5 were associated with the conversion of serine to O-phosphoserine that can connect with the acidic mineral-binding motifs, contributing to the interfacial adhesion of mussel byssus to the calcareous substrates (Waite 2001; Zhao and Waite 2006). Phosphorylated proteins were also identified from the uncured cement of the fouling barnacle *Amphibalanus amphitrite*, which were further located in the organic matrix of base plate and capillary ducts, demonstrating that these phosphorylated proteins can form strong ionic bonds with underwater minerals and induce the mineralization of calcium carbonate (Dickinson et al. 2016). Cement was usually used to build the mineralized tubes of the sandcastle worm *Phragmatopoma californica*. Pc-3 was one of the three adhesive proteins with higher polarity in worm cement. It was rich in serine residues (60–90 mol%) and most of which were phosphorylated (Zhao et al. 2005). It has been suggested that there were complex interactions among the phosphorylated serine of adhesive proteins, the free Ca^{2+} in surrounding waters, and the submersed calcium substrates during the underwater adhesion of marine fouling organisms. A thrombospondin-containing byssal protein TSP-1 in the pearl oyster *Pinctada fucata* could aggregate and self-assemble through the interactions between Ca^{2+} and phosphorylated serine or vWF domains in this protein, promoting the formation of byssus and binding ability of byssus to calcium substrates. In addition, the phosphorylation site of adhesive proteins was also supposed to be of strong electrostatic attraction with Ca^{2+}, forming the rigid structures of silks (Liu et al. 2016; George and Veis 2008). Overall, the sequence features of APAP-2 suggest that it may function as an adhesive protein taking part in the interfacial adhesion between the papillae of *C.robusta* and underwater substrates by regulating the interaction of Ca^{2+}, phosphorylated amino acids, and conserved domains. This conclusion was further supported by the evidence that the up-regulated terms/pathways related to Ca^{2+} transport and serine phosphorylation were significantly enriched in papillae (Fig. 2). Importantly, the recombinant protein APAP-2 exhibits strong adhesive abilities to the surfaces of various materials in our surface coating experiments (Fig. 4a).

Conclusion

By using micro-dissection and micro-transcriptome sequencing technologies, we obtained a gene pool that was highly expressed in papillae, the fouling organs of ascidian larvae. The terms/pathways related to neural recognition, environmental perception, metabolism, and ion transport were significantly enriched in functional analyses, confirming the important roles of these processes during the papillary adhesion of ascidian larvae. In addition, two candidate adhesive proteins APAP-1 and APAP-2 were identified, expressed, and purified *in vitro*, and functionally, they were proved to be a cohesive protein and interfacial protein, respectively, in the papillary adhesion. Multiple lines of evidence in our study clearly illustrate that papillae are adhesive structures in ascidian larvae with multiple functions of substrate recognition, environmental perception, and proteins synthesis and secretion.

Declarations

Acknowledgements Great thanks to Profs. Zunchun Zhou and Bei Jiang for their assistance in ascidian collection.

Author Contributions Conceptualization: A.Z., S.L.; Methodology: J.C., X.L.; Formal analysis: J.C.; Investigation: J.C., R.F.; Writing-original draft: J.C.; Writing-review & editing: A.Z., S.L., X.H.; Supervision: A.Z., S.L.; Project administration: A.Z., S.L.; Funding acquisition: A.Z., S.L.

Funding This work was supported by the National Natural Science Foundation of China (Grant Nos. 42076098 and 32061143012), Youth Innovation Promotion Association, Chinese Academy of Sciences (Grant No. 2018054).

Data Availability All the raw sequencing data of transcriptome sequencing were deposited in the National Centre for Biotechnology Information (NCBI) under the accession number (SUB10810372).

Compliance with Ethical Standards

Conflict of Interest The authors declare that they have no conflict of interest.

References

1. Adams CM (2011) Biofouling in marine molluscan shellfish aquaculture: A survey assessing the business and economic implications of mitigation. J World Aquacult Soc 42: 242–252
2. Aldred N, Clare AS (2014) Mini-review: Impact and dynamics of surface fouling by solitary and compound ascidians. Biofouling 30: 259–270

3. Bannister J, Sievers M, Bush F, Bloecher N (2019) Biofouling in marine aquaculture: a review of recent research and developments. Biofouling 35: 631–648
4. Bolger AM, Lohse M, Usadel B (2014) Trimmomatic: a flexible trimmer for Illumina sequence data. Bioinformatics 30: 2114–2120
5. Blum JC, Chang AL, Liljesthröm M, Schenk ME, Steinberg MK, Ruiz GM (2007) The non-native solitary ascidian *Ciona intestinalis* (L.) depresses species richness. J Exp Mar Biol and Ecol 342: 5–14
6. Caicci F, Zaniolo G, Burighel P, Degasperi V, Gasparini F, Manni L (2010) Differentiation of papillae and rostral sensory neurons in the larva of the ascidian *Botryllus schlosseri* (Tunicata). J Comp Neurol 518: 547–566
7. Cao C, Lemaire LA, Wang W, Yoon PH, Choi YA, Parsons LR, Matese JC, Wang W, Levine M, Chen K (2019) Comprehensive single-cell transcriptome lineages of a proto-vertebrate. Nature 571: 349–354
8. Castilla JC, Guiñez R, Caro AU, Ortiz V (2004) Invasion of a rocky intertidal shore by the tunicate *Pyura praeputialis* in the Bay of Antofagasta, Chile. Proc Natl Acad Sci USA 101: 8517–8524
9. Chase AL, Dijkstra JA, Harris LG (2016) The influence of substrate material on ascidian larval settlement. Mar Pollut Bull 106: 35–42
10. Chaw KC, Birch WR (2009) Quantifying the exploratory behaviour of *Amphibalanus amphitrite* cyprids. Biofouling 25: 611–619
11. Chen CJ, Chen H, Zhang Y, Thomas HR, Frank MH, He YH, Xia R (2020) TBtools: An integrative toolkit developed for interactive analyses of big biological data. Mol Plant 13: 1194–1202
12. Cloney RA (1977) Larval adhesive organs and metamorphosis in ascidians. J Cell Tissue Res 183: 423–444
13. Davis MH, Davis ME (2010) The impact of the ascidian *Styela clava* Herdman on shellfish farming in the Bassin de Thau, France. J Appl Ichthyol 26: 12–18
14. de With G (2018) Polymer coatings: A guide to chemistry, characterization and selected applications. Wiley, New York
15. Dickinson GH, Yang X, Wu F, Orihuela B, Rittschof D, Beniash E (2016) Localization of phosphoproteins within the barnacle adhesive interface. Biol Bull 230: 233–242
16. D' Aniello S, D' Aniello E, Locascio A, Memoli A, Corrado M, Russo MT, Aniello F, Fucci L, Brown ER, Branno M (2006) The ascidian homolog of the vertebrate homeobox gene Rx is essential for ocellus development and function. Differentiation 74: 222–234
17. Fitridge I, Dempster T, Guenther J, de Nys R (2012) The impact and control of biofouling in marine aquaculture: a review. Biofouling 28: 649–669
18. Fujikawa T, Munakata T, Kondo S-I, Satoh N, Wada S (2010) Stress response in the ascidian *Ciona intestinalis*: transcriptional profiling of genes for the heat shock protein 70 chaperone system under heat stress and endoplasmic reticulum stress. Cell Stress Chaperones 15: 193–204
19. George A, Veis A (2008) Phosphorylated proteins and control over apatite nucleation, crystal growth, and inhibition. Chem Rev 108: 4670–4693
20. Groppelli S, Pennati R, Scarì G, Sotgia C, Bernardi FD (2003) Observations on the settlement of *phallusia mammillata* larvae: Effects of different lithological substrata. Ital J Zool 70: 321–326
21. Hartig SM (2013) Basic image analysis and manipulation in ImageJ. Curr Protoc Mol Biol 102: 14.15.1-14.15.12
22. Hennebert E, Wattiez R, Demeuldre M, Ladurner P, Hwang DS, Waite JH, Flammang P (2014) Sea star tenacity mediated by a protein that fragments, then aggregates. Proc Natl Acad Sci USA 111: 6317–6322
23. Hirai S, Hotta K, Kubo Y, Nishino A, Okabe S, Okamura Y, Okada H (2017) AMPA glutamate receptors are required for sensory-organ formation and morphogenesis in the basal chordate. Proc Natl Acad Sci USA 114: 3939–3944
24. Hirose E, Akahori M (2004) Comparative morphology of the stolonic vessel in a didemnid ascidian and some related tissues in colonial ascidians. Zool Sci 21: 445–455
25. Horie T, Nakagawa M, Sasakura Y, Kusakabe TG (2009) Cell type and function of neurons in the ascidian nervous system. Dev Growth Differ 51: 207–220
26. Hotta K, Mitsuhara K, Takahashi H, Inaba K, Oka K, Gojobori T, Ikeo K (2007) A web-based interactive developmental table for the ascidian *Ciona intestinalis*, including 3D real-image embryo reconstructions: I. From fertilized egg to hatching larva. Dev Dyn 236: 1790–1805
27. Hwang DS, Zeng H, Masic A, Harrington MJ, Israelachvili JN, Waite JH (2010) Protein- and metal-dependent interactions of a prominent protein in mussel adhesive plaques. J Biol Chem 285: 25850–25858
28. Imai JH, Meinertzhagen IA (2007a) Neurons of the ascidian larval nervous system in *Ciona intestinalis*: I. Central nervous system. J Comp Neurol 501: 316–334
29. Imai JH, Meinertzhagen IA (2007b) Neurons of the ascidian larval nervous system in *Ciona intestinalis*: II. Peripheral nervous system. J Comp Neurol 501: 335–352
30. Kamino K (2001) Novel barnacle underwater adhesive protein is a charged amino acid-rich protein constituted by a Cys-rich repetitive sequence. Biochem J 356: 503–507
31. Kamino K, Inoue K, Maruyama T, Takamatsu N, Harayama S, Shizuri Y (2000) Barnacle cement proteins: Importance of disulfide bonds in their insolubility. J Biol Chem 275: 27360–5
32. Kamino K, Nakano M, Kanai S (2012) Significance of the conformation of building blocks in curing of barnacle underwater adhesive. FEBS J 279: 1750–1760
33. Kim D, Langmead B, Salzberg SL (2015) HISAT: a fast spliced aligner with low memory requirements. Nat Methods 12: 357–360
34. Kon-ya K, Miki W (1994) Effects of environmental factors on larval settlement of the barnacle *Balanus amphitrite* reared in the laboratory. Fish Sci 60: 563–565
35. Lambert G (2007) Invasive sea squirts: A growing global problem. J Exp Mar Biol Ecol 342: 3–4

36. Li SG, Huang XN, Chen YY, Li X, Zhan AB (2019) Identification and characterization of proteins involved in stolon adhesion in the highly invasive fouling ascidian *Ciona robusta*. Biochem Biophys Res Commun 510: 91–96
37. Li X, Li SG, Cheng JW, Fu RY, Zhan AB (2021a) Proteomic response to environmental stress in the stolon of a highly invasive fouling ascidian. Front Mar Sci 8: 761628
38. Li X, Li SG, Huang XN, Chen YY, Cheng JW, Zhan AB (2021b) Protein-mediated bioadhesion in marine organisms: A review. Mar Environ Res 170: 105409
39. Liao Y, Smyth GK, Shi W (2014) FeatureCounts: an efficient general purpose program for assigning sequence reads to genomic features. Bioformatics 30: 923–930
40. Liu C, Xie LP, Zhang RQ (2016) Ca^{2+} mediates the self-assembly of the foot proteins of *Pinctada fucata* from the nanoscale to the microscale. Biomacromolecules 17: 3347–3355
41. Livak KJ, Schmittgen TD (2001) Analysis of relative gene expression data using real-time quantitative PCR and the $2^{-\Delta\Delta CT}$ method. Methods 25: 402–408
42. Love MI, Huber W, Anders S (2014) Moderated estimation of fold change and dispersion for RNA-seq data with DESeq2. Genome Biol 15: 550
43. Madin J, Ching CV (2015) In: Mustafa S, Shapawi R (ed) Aquaculture Ecosystems: Adaptability and Sustainability. Wiley, New York
44. Marsden JE, Lansky D (2011) Substrate selection by settling zebra mussels, *Dreissena polymorpha*, relative to material, texture, orientation, and sunlight. Can J Zool 78: 787–793
45. Maruzzo D, Conlan S, Aldred N, Clare AS, Høeg JT (2011) Video observation of surface exploration in cyprids of *Balanus amphitrite*: the movements of antennular sensory setae. Biofouling 27: 225–239
46. Matsunobu S, Sasakura Y (2015) Time course for tail regression during metamorphosis of the ascidian *Ciona intestinalis*. Dev Biol 405: 71–81
47. Moussa FM, Hisijara IA, Sondag GR, Scott EM, Frara N, Abdelmagid SM, Safadi FF (2014) Osteoactivin promotes osteoblast adhesion through HSPG and αvβ1 integrin. J Cell Biochem 115: 1243–1253
48. Opell BD, Bruba CM, Deva PD, Kin MHY, Rivas MX, Elmore HM, Hendricks ML (2019) Linking properties of an orb - weaving spider's capture thread glycoprotein adhesive and flagelliform fiber components to prey retention time. Ecol Evol 9: 9841–9854
49. Pang ZP, Südhof TC (2010) Cell biology of Ca^{2+}-triggered exocytosis. Curr Opin Cell Biol 22: 496–505
50. Pennati R, Zega G, Groppelli S, Bernardi FD (2007) Immunohistochemical analysis of the adhesive papillae of *Botrylloides leachi* (Chordata, Tunicata, Ascidiacea): Implications for their sensory function. Ital J Zool 74: 325–329
51. Picelli S, Garidani OR, Björklund ÅK, Winberg G, Sagasser S, Sandberg R (2014) Full-length RNA-seq from single cells using Smart-seq2. Protocol 9: 171–181
52. Prendergast GS (2009) In: Dürr S, Thomason JC (ed) Biofouling. Wiley, New York
53. Rocha M, Antas P, Castro LFC, Campos A, Vasconcelos V, Pereira F, Cunha I (2019) Comparative Analysis of the Adhesive Proteins of te Adult Stalked Goose Barnacle Pollicipes pollicipes (Cirripedia: Pedunculata). Mar Biotechnol 21: 38–51
54. Salta M, Wharton JA, Stoodley P, Dennington SP, Goodes LR, Werwinski S, Mart U, Wood RJK, Stokes KR (2010) Designing biomimetic antifouling surfaces. Philos Trans A Math Phys Eng Sci 368: 4729–4754
55. Sarosiek J, Mizuta K, Slomiany A, Slomiany BL (1988) Effect of deglycosylation on gastric mucin viscosity and acid impedance. Ann N Y Acad Sci 529: 254–256
56. Satou Y, Nakamura R, Yu D, Yoshida R, Hamada M, Fujie M, Hisata K, Takeda H, Satoh N (2019) A nearly complete genome of *Ciona intestinalis* type A (*C. robust*a) reveals the contribution of inversion to chromosomal evolution in the genus *Ciona*. Genome Biol Evol 11: 3144–3157
57. Silverman HG, Roberto FF (2007) Understanding Marine Mussel Adhesion. Mar Biotechnol 9: 661–681
58. Suhre MH, Gertz M, Steegborn C, Thomas S (2014) Structural and functional features of a collagen-binding matrix protein from the mussel byssus. Nat Commun 26: 3392
59. Svane I, Young CM (1989). The ecology and behaviour of ascidian larvae. Oceanogr Mar Biol Ann Rev 27: 45–90
60. Torrence SA, Cloney RA (1983) Ascidian larval nervous system: Primary sensory neurons in adhesive papillae. Zoomorpgology 102: 111–123
61. Tsuda M, Kawakami I, Shiraishi S (2003) Sensitization and habituation of the swimming behavior in ascidian larvae to light. Zool Sci 20: 13–22
62. Ueki T, Koike K, Fukuba I, Yamaguchi N (2018) Structural and mass spectrometric imaging analyses of adhered tunic and adhesive projections of solitary ascidians. Zool Sci 35: 535–547
63. Urushida Y, Nakano M, Matsuda S, Inoue N, Kanai S, Kitamura N, Nishino T, Kamino K (2007) Identification and functional characterization of a novel barnacle cement protein. FEBS J 274: 4336–4346
64. Waite JH (2001) Polyphosphoprotein from the Adhesive Pads of *Mytilus edulis*. Biochemistry 40: 2887–2893
65. Wickham H, Chang W, Henry L (2016) ggplot2: Elegant graphics for data analysis. New York (NY): Springer
66. Zeng F, Wunderer J, Salvenmoser W, Ederth T, Rothbächer U (2019a) Identifying adhesive components in a model tunicate. Philos Trans R Soc B 374: 20190197
67. Zeng F, Wunderer J, Salvenmoser W, Hess MW, Ladurner P, Rothbächer U (2019b) Papillae revisited and the nature of the adhesive secreting collocytes. Dev Biol 448: 183–198
68. Zhan AB, Briski E, Bock DG, Ghabooli S, MacIsaac HJ (2015) Ascidians as models for studying invasion success. Mar Biol 162: 2449–2470
69. Zhao H, Waite JH (2006) Linking adhesive and structural proteins in the attachment plaque of *Mytilus californianus*. J Biol chem 281: 26150–26158

70. Zhao H, Sun CJ, Stewart RJ, Waite H (2005) Cement proteins of the tube-building polychaete *Phragmatopoma californica*. J Biol chem 280: 42938–42944

Tables

Table 1 The functional genes involved in papillary adhesion in the ascidian *Ciona robusta* screened by micro-transcriptome sequencing technique

Category	Gene ID	Gene description	Molecular size (kDa)	Amino acid composition (top three)	Domain	log_2 (fold change)	Q-value
Papilla adhesive proteins	KY.Chr1.200.v3.ND3-3	SCO-spondin	116.29	Ser12.8%,Cys11.5%,Thr7.1%	TSP-1,vWC_def	4.54	7.01E-05
	KY.Chr11.377.v2.ND2-1	spondin 2	18.54	Gly12.9%,Lys11.1%,Ser9.9%	TSP-1	7.58	9.04E-05
	KY.Chr2.475.v2.SL2-1	fibronectin 1	49.41	Arg11%,Val8.2%,Thr7.5%	FN1,FOLN,vWC	3.16	1.52E-04
	KY.Chr11.146.v1.SL1-1	delta like non-canonical Notch ligand 2	53.14	Thr11.3%,Gly8.8%,Cys8.4%	EGF,EGF_CA,EGF_like	2.66	1.61E-04
	KY.Chr10.1268.v1.ND1-1	chordin like 1	49.8	Ser12%,Cys7.9%,Arg7.4%	vWC	2.07	2.94E-04
	KY.Chr10.1028.v1.nonSL5-1	sushi, von Willebrand factor type A, EGF and pentraxin domain containing 1	34.88	Cys11.8%,Glu10.2%,Gly9.6%	EGF,EGF_CA,EGF_like,GLA	3.52	2.24E-02
Neural perception-related proteins	*KY.Chr1.1186.v2.ND1-2	opsin 1, long wave sensitive	44.36	Leu10.4%,Val10.2%,Ile7.6%	Pfam:7tm_1	5.40	2.32E-05
	*KY.Chr7.1150.v1.ND1-1	G protein-coupled receptor 84	31.06	Ser10.3%,Lys9.6%,Leu8.5%	Pfam:7tm_1	2.69	8.11E-04

Figures

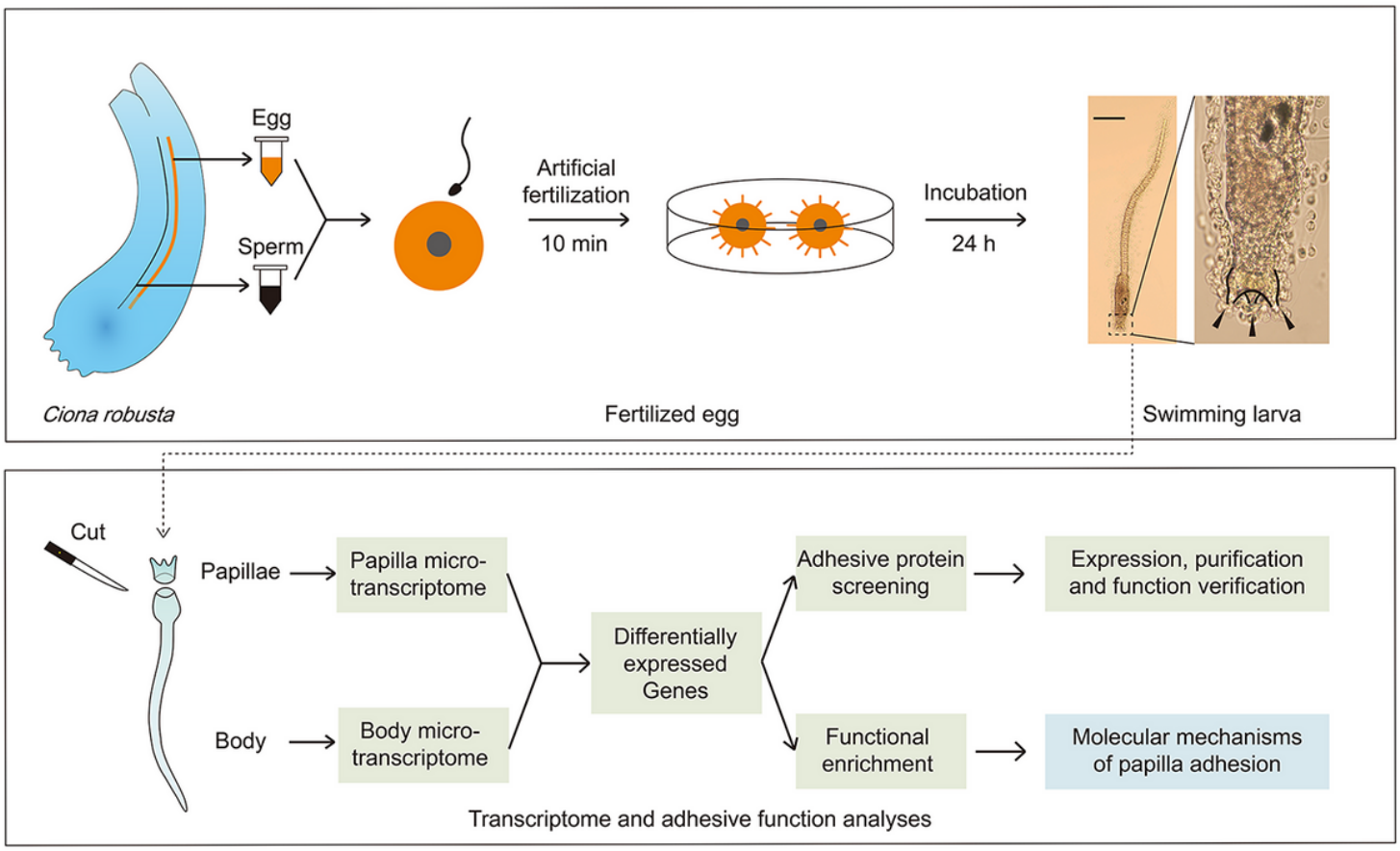

Figure 1

Schematic experimental design for molecular functional analyses of larval adhesion in the highly fouling ascidian, *Ciona robusta*. Swimming larvae of the ascidian *C. robusta* were obtained by artificial fertilization *in vitro*. The dashed box at swimming larva stage shows the location of papillae. The papillae are enlarged, and the arrows show three papillae arranged in a triangular position prior to the larval head. The shape of papillae is highlighted by black curves. Scale bar = 100 μm

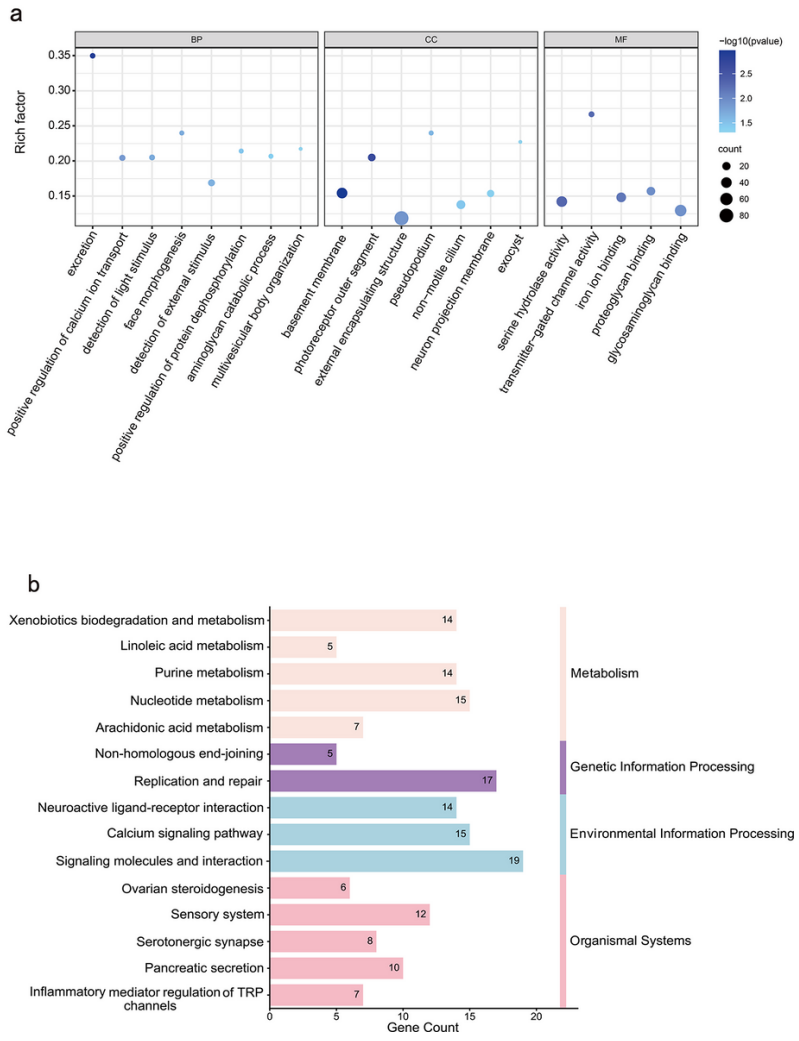

Figure 2

Gene ontology (GO) and Kyoto encyclopedia of genes and genomes (KEGG) enrichment analyses for the differentially expressed genes (DEGs) obtained from the papillae and body transcriptomes of the fouling ascidian *Ciona robusta*. **a** The significantly enriched GO terms. **b** The significantly enriched KEGG pathways. BP: biological process. CC: cellular component. MF: molecular function

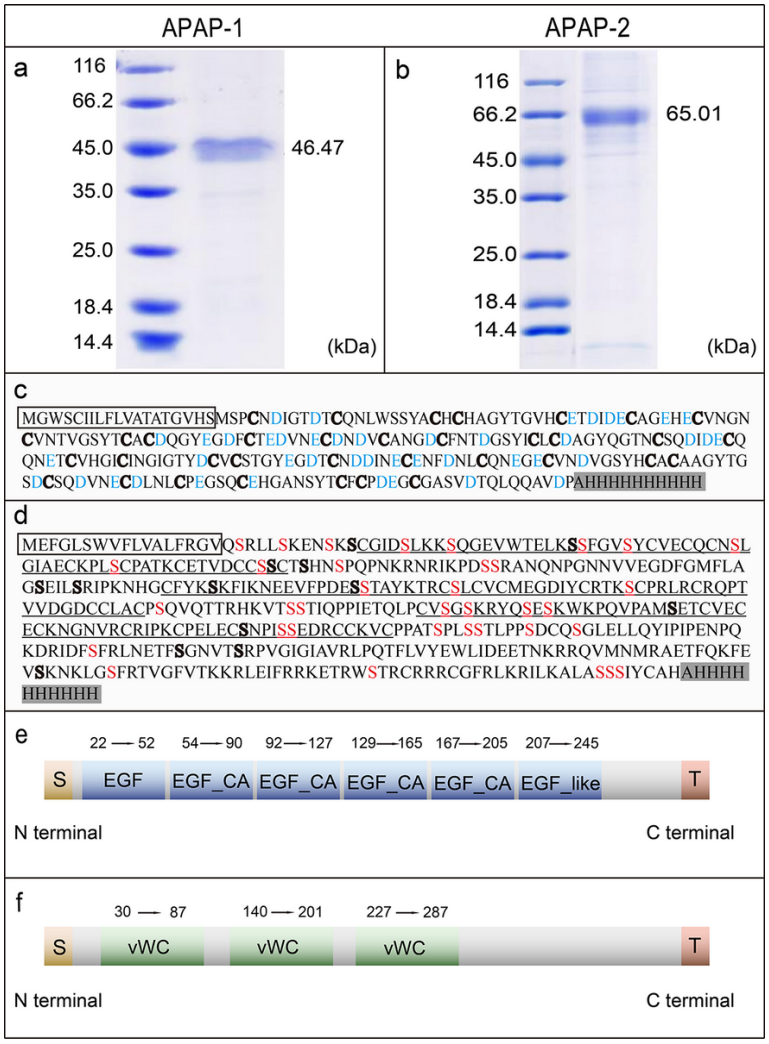

Figure 3

Expression, purification, and sequence analyses of ascidian papilla adhesive protein 1 and 2 (APAP-1 and APAP-2). **a** and **b** The sodium dodecyl sulphate-polyacrylamide gel electrophoresis (SDS-PAGE) results of APAP-1 and APAP-2. **c** The amino acid sequence of APAP-1. Letters with frame show the signal peptide, blue letters illustrate amino acids with negative charge, bolded letters show cysteine, and shaded letters show C-terminal decahistidine tag. **d** The amino acid sequence of APAP-2. Bolded red letters show serine, and red letters illustrate phosphorylated serine. vWC = von Willebrand factor type C domain (underlined letters). **e** The conserved domains of APAP-1. EGF = Epidermal Growth Factor. EGF_like = EGF-like domain. S = Signal peptide. T = histidine Tag. **f** The conserved domains of APAP-2. The number range above each domain represents the position in the amino acid sequence of APAP-1 and APAP-2

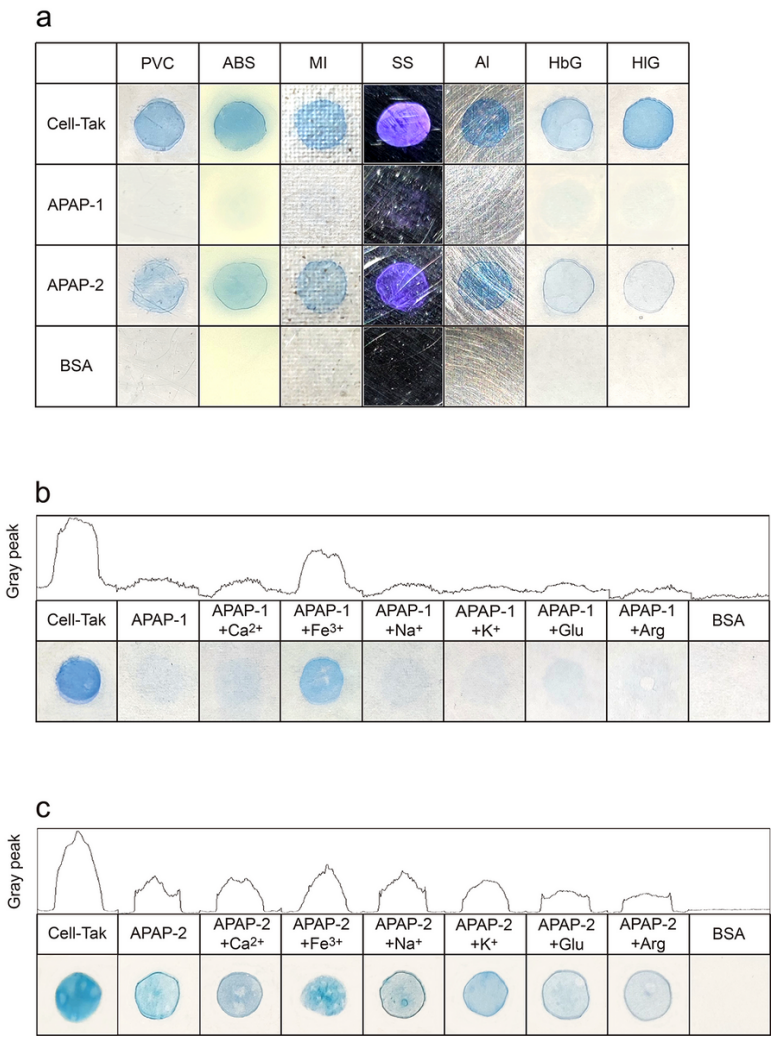

Figure 4

Surface coating and gray analysis for the adhesive abilities of ascidian papilla adhesive protein 1 and 2 (APAP-1 and APAP-2). The peaks represent the gray values of the spots color. Bovine serum albumin (BSA) was used as negative control, while a commercial adhesive protein mixture (Cell-Tak) was used as positive control. **a** Adhesive ability tests for APAP-1 and APAP-2 on different material surfaces - PVC: polyvinyl chloride. ABS: acrylonitrile-butadiene-styrene plastic. MI: mica. SS: stainless steel. Al: aluminum. HbG: hydrophobic glass. HIG: hydrophilic grass. **b** Effects of different metal ions and amino acids on the adhesive ability of APAP-1 to PVC. **c** Effects of different metal ions and amino acids on the adhesive ability of APAP-2 to PVC

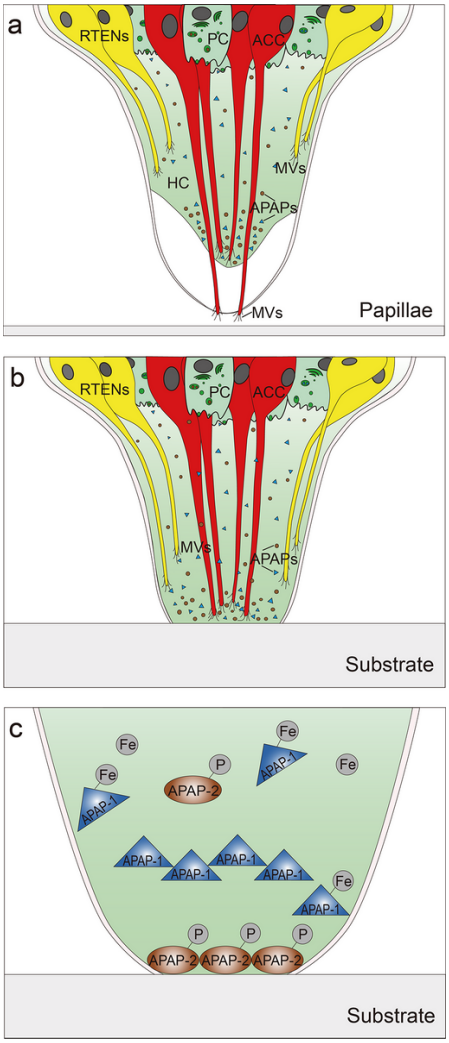

Figure 5

The diagrammatic presentation of the molecular mechanisms underlying papillary adhesion in the fouling ascidian *Ciona robusta*. **a** The papillary structure of swimming larva. The axial columnar cells of *C. robusta* papillae with microvillus can recognize substrate surface. Meanwhile, the ascidian papilla adhesive proteins (APAPs) are synthesized by papillary collocytes and secreted to hyaline cap. **b** and **c** Once the substrate is suitable for adhesion, the APAPs stored in hyaline cap will be rapidly released. APAP-1 is released and acts as a cohesive protein by binding metal ions. APAP-2 is released to the interface between papillae and substrate surface, playing important role in interfacial adhesion by regulating the interactions among metal ions, phosphorylated amino acids and conserved domains. RTENs: rostral trunk epidermal neurons. PC: papillary collocytes. ACC: axial columnar cells. HC: hyaline cap. MVs: microvillus. APAPs: ascidian papilla adhesive proteins. Fe: iron ion. P: phosphorylated

Supplementary Files

This is a list of supplementary files associated with this preprint. Click to download.

- SupplementaryMaterials.pdf
- TableS3.xlsx